

[Re] Multiple dynamical modes of thalamic relay neurons: rhythmic bursting and intermittent phase-locking

Georgios Detorakis¹

¹ Department of Cognitive Sciences, UC Irvine, CA, USA

gdetorak@uci.edu

gdetor@protonmail.com

Editor

Tiziano Zito

Reviewers

Hans Ekkehard Plesser
Andrew Davison

Received May, 9, 2016

Accepted Aug, 29, 2016

Published Sep, 7, 2016

Licence [CC-BY](#)

Competing Interests:

The authors have declared that no competing interests exist.

 [Article repository](#)

 [Code repository](#)

A reference implementation of

→ *Multiple dynamical modes of thalamic relay neurons: rhythmic bursting and intermittent phase-locking*, Wang, X-J, *Neuroscience*, 59(1), pg. 21–31, 1994.

Introduction

The present paper replicates a neuron model for thalamocortical relay neurons, proposed by X-J Wang, [4]. The model is conductance-based and takes advantage of the interplay between a T-type calcium current and a non-specific cation sag current and thus, it is able to generate spindle and delta rhythms. Another feature of this model is the presence of an intermittent phase-locking phenomenon where action potentials of sodium take place in a non-periodic manner, despite the fact that they are phase-locked to the periodic input current. Finally, the model is capable of generating tonic spike patterns. The source code for replicating Wang's model is written in Python (Numpy, Scipy, Matplotlib, and Scikit-image).

Methods

In this section, a detailed description of the model is given following the paradigm of Nordlie et al, [3]. To this end, a description of the model's equations, parameters, and inputs are given in the form of tables.

Table 1 and 2 provide a description of the model and information about simulations duration and time steps, respectively. Table 3 gives a glimpse of the input signals used in this work and Table 4 introduces the equations of the model. Table 5 summarizes all the parameters used in this work.

The neuron model is conductance-based, consisting of four differential equations describing the dynamics of membrane potential and the kinetics of a T-Type calcium current, a Sag current channel and a Potassium channel. The rest of the currents are described by algebraic equations.

Before proceeding to the simulations we introduce a few details regarding the source code and the integration method which should be accurate and fast enough. The implementation is a Python class (Python 3.5.1), which uses Numpy (version 1.10.4), Scipy (version 0.17.0), Matplotlib (1.5.1) and Scikit-image (version 0.12.3) packages. The numerical integration is carried out using the *ode* method of Scipy *integrate* package. Three different methods were tested in this work (*dopri5*, *Adams*, *BDF*, [1]).

Model Summary	
Populations	No population – one neuron model
Topology	–
Connectivity	–
Neuron Model	Hodgkin-Huxley conductance-based
Channel Models	
Synapse Model	–
Plasticity	–
Input	Constant current or periodic rectangular pulses
Measurements	Membrane potential, channels activation, phase plane

Table 1: Summary of the model

Dopri5 is the closest numerical method to the one used by [4] (fifth-order adaptive size Runge-Kutta method). The user of the present implementation can choose one of the three methods at the stage of class instantiating. For all three methods we measured spike times, membrane potential amplitudes and the coefficient of variation using as threshold value 0 mV. *Dopri5* and *Adams* methods differ in one spike event time whilst *dopri5* and *BDF* have a difference of 37 spike events. However, all three methods (*dopri5*, *Adams* and *BDF*) have the same $CV \simeq 2.3608$. The most striking difference is found for the amplitude of membrane potential. Figure 1 A shows the membrane potential (in mV) produced by *dopri5* plotted against the membrane potential generated by *Adams* method. Figure 1 B shows the membrane potential of a simulation using *dopri5* against another using *BDF*. The *Adams* method has less differences in amplitude from *dopri5* than *BDF*. Therefore, we decided to use the *Adams* method since it runs faster than *dopri5*.

Figure	Simulated Time	
	Simulation Time (s)	Integration Step (ms)
1	6	0.05
2	$15 \times \text{period}, 5$	0.05
3	6	0.05
4	1.5, 1, 1	0.05
5	5	0.05
6	5	0.05
7	40, 20	0.05

Table 2: Simulated Time

All simulations ran on a Dell OptiPlex 7040, equipped with a sixth generation i7 processor, 8 GB of physical memory and running Arch Linux. The total execution time of all simulations was 526 minutes and the peak consumed memory was 465 MB¹. All the parameters used in this work are given in Table 5.

Results

We simulated the model described in Table 4 using parameters given in Table 5 and the corresponding inputs (see Table 3). First, we examined the response of the present implementation to rhythmic hyperpolarization. In [4] this is illustrated in Wang's Fig 1. Thus, we applied a periodic current pulse of $-1 \mu\text{A}/\text{cm}^2$ amplitude at several different frequencies ($\frac{1}{P_0}$ is the frequency in Hz and P_0 is the corresponding period in ms) ranging from 0.1 Hz to 15 Hz with a resolution (discretization) of 100 samples.

¹Python memory profiler used (https://pypi.python.org/pypi/memory_profiler).

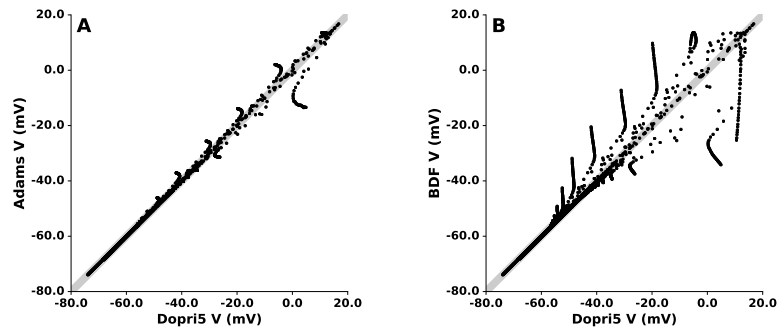


Figure 1: Amplitude differences The membrane potential (mV) is generated using *dopri5* integration method and is plotted (black dots) against (A) the one generated by *Adams* method and (B) *BDF* method. The light shaded diagonal area indicates a 2 mV difference.





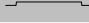


Figure	Type	Input			
		Form	Frequency ($\frac{1}{P_0}$, Hz)	Duration (p , ms)	Amplitude ($\mu\text{A}/\text{cm}^2$)
Figure 1	Constant		—	—	−0.6
Figure 2	Periodic		5, 10	10, 40	−1.0 +3.0 3 0.0 −0.45 −0.455 −0.47 −0.55 −0.6 −0.8 −1.3 −1.4 −2.1 −1.25
Figure 3	Constant		—	—	0.25 −0.47 −0.95
Figure 4	Pulse/Constant		—	100	[−2, 0] [−2, 0]
Figure 5	Constant		—	—	
Figure 6	Constant		—	—	
Figure 7	Constant		—	—	

Table 3: Description of the applied current I_{app}

Neuron Model	
Name	Thalamocortical relay neuron
Type	Conductance-based neuron
Membrane Potential	$C_m \frac{dV(t)}{dt} = -I_T - I_h - I_{Na} - I_K - I_{Na(P)} - I_L + I_{app}$
T-Type Calcium Current (I_T)	$I_T = g_T \cdot s_\infty^3(V) \cdot h \cdot (V - V_{Ca})$
	$s_\infty(V) = \frac{1}{1 + \exp(-\frac{V+65}{7.8})}$
	$\frac{dh(t)}{dt} = \phi_h \frac{h_\infty(V) - h}{\tau_h(V)}$
	$h_\infty(V) = \frac{1}{1 + \exp(\frac{V-\theta_h}{k_h})}$
	$\tau_h(V) = h_\infty \exp(\frac{V + 162.3}{17.8}) + 20$
Sag Current (I_h)	$I_h = g_h \cdot H^2 \cdot (V - V_h)$
	$H_\infty(V) = \frac{1}{1 + \exp(\frac{V+69}{7.1})}$
	$\frac{dH(t)}{dt} = \phi_H \frac{H_\infty(V) - H}{\tau_H(V)}$
Hodgkin-Huxley Currents (I_K) and (I_{Na})	$I_K = g_K \cdot n^4 \cdot (V - V_K)$
	$\frac{dn(t)}{dt} = \phi_n \frac{n_\infty(V) - n(t)}{\tau_n(V)}$
	$n_\infty(\sigma_K, V) = \frac{\alpha_n(\sigma_K, V)}{\alpha_n(\sigma_K, V) + \beta_n(\sigma_K, V)}$
	$\tau_n(\sigma_K, V) = \frac{1}{\alpha_n(\sigma_K, V) + \beta_n(\sigma_K, V)}$
	$\alpha_n(\sigma_K, V) = \frac{-0.01(V + 45.7 - \sigma_K)}{\exp(-0.1(V + 45.7 - \sigma_K)) - 1}$
	$\beta_n(\sigma_K, V) = 0.125 \exp(-\frac{V + 55.7 - \sigma_K}{80})$
	$I_{Na} = g_{Na} \cdot m_\infty^3(\sigma_{Na}, V) \cdot (0.85 - n) \cdot (V - V_{Na})$
	$m_\infty(V) = \frac{\alpha_m(\sigma_{Na}, V)}{\alpha_m(\sigma_{Na}, V) + \beta_m(\sigma_{Na}, V)}$
	$\alpha_m(\sigma_{Na}, V) = -0.1 \frac{V + 29.7 - \sigma_{Na}}{\exp(-0.1(V + 54.7 - \sigma_{Na})) - 1}$
	$\beta_m(\sigma_{Na}, V) = 4 \exp(-\frac{V + 54.7 - \sigma_{Na}}{18})$
Persistent Sodium Currents ($I_{Na(P)}$)	$I_{Na(P)} = g_{Na(P)} \cdot m_\infty^3(\sigma_{Na(P)}, V) \cdot (V - V_{Na})$
Leak Current (I_L)	$I_L = g_L \cdot (V - V_L)$

Table 4: Description of the neuron model

Model Parameters							
Figure	V_0 (mV)	g_T (mS/cm ²)	θ_h (mV)	k_h (mV ⁻¹)	σ_{Na} (mV)	g_L (mS/cm ²)	V_L (mV)
1	-74	1	-79	5	6	0.12	-70
2	-74	0.3	-81	6.25	3	0.1	-72
3	-74	1	-79	5	6	0.12	-70
4	-72/-64	1.0	-79	5	6	0.12	-70
5	-74	1.0	-75	5	6	0.08	-70
6	-74	1/0.7	-79	5	6	0.12/0.04	-70
7	-72	0.3/0.25	-81	6.25	3	0.1	-72
Common Parameters							
$C_m = 1 \mu\text{F}/\text{cm}^2$, $\phi_h = 2$, $V_{Ca} = 120 \text{ mV}$, $\phi_H = 1$, $g_h = 0.04 \text{ mS}/\text{cm}^2$, $V_h = -40 \text{ mV}$, $g_K = 30 \text{ mS}/\text{cm}^2$, $V_K = -80 \text{ mV}$, $g_{Na} = 42 \text{ mS}/\text{cm}^2$, $V_{Na} = 55 \text{ mV}$, $\phi_n = \frac{200}{7}$, $\sigma_K = 10 \text{ mV}$, $V_{Na(P)} = 55 \text{ mV}$, $\sigma_{Na(P)} = -5 \text{ mV}$, $g_{Na(P)} = 9 \text{ mS}/\text{cm}^2$							

Table 5: Simulation Parameters

The same number of samples used for discretizing the duration (ON/OFF) of the pulse for each frequency. The ON duration of a pulse is defined by the value of p and the OFF duration as $P_0 - p$.

The results are depicted in Figure 2. Upper panel shows two different simulations of the present implementation at specific frequencies (5, 0.5 Hz) and ratios p/P_0 (0.6, 0.6), respectively (following the upper panels of Fig 1 in [4]). The results in Figure 2 are comparable to the ones presented in [4] and the timescales are exactly the same (400 ms for the left sub-panel and 4 s for the second one). However, numbers regarding pulse ON duration (p) in Wang's Fig 1 are possibly an error. As an example, assume that the frequency is $\frac{1}{P_0} = 5 \text{ Hz}$ and $\frac{p}{P_0} = 0.6$ then the pulse ON duration must be $p = 120 \text{ ms}$ and not 160 ms (that is reported in [4]). Bottom panel illustrates the total results of 100×100 simulations. In order to create this figure, we counted the number of spikes, both supra- and sub-threshold ones, generated per pulse and then we computed the mean (this procedure is not described in full detail in [4], however more details can be found in [2]). Figure 2 differs from the one in [4], to the point that the shaded area that contains an average number of spikes below 1.0 (but not zero) is larger than in [4]. Unfortunately, there are not enough details regarding Fig 1 in [4] to make a faithful reproduction of that figure.

The next simulation investigated the transition from subthreshold to bursting oscillations via chaos. This is illustrated in Fig 3 in [4]. In this case a steady current is applied to the model described in Table 4. In [4] Wang used eleven different amplitudes for the constant current in order to explore the model's behavior repertoire. Hence,

$$I_{app} = 3.0, 0.0, -0.45, -0.455, -0.47, -0.55, -0.6, -0.8, -1.3, -1.4, -2.0 \mu\text{A}/\text{cm}^2.$$

The results for these simulations are depicted in Figure 3. In this case, there was no difference between the present implementation and the original one.

[4] has showed that the current model expresses a hysteresis (see Wang's Fig 4). In order to reproduce that case we simulated the model using a constant external current I_{app} . The simulation starts by applying a current with an amplitude of $-0.433 \mu\text{A}/\text{cm}^2$ and continues by increasing the amplitude up to $-0.55 \mu\text{A}/\text{cm}^2$. At every iteration, sub- and/or supra-threshold activity of the membrane potential is detected. The results are given in Figure 4 A. In addition, the model expresses a bistability. This was tested by applying the same protocol as in [4]. Thus first a brief pulse (for 100 ms) of $0.25 \mu\text{A}/\text{cm}^2$ (black line in Figure 4 C) or $-1.2 \mu\text{A}/\text{cm}^2$ (gray line in Figure 4 C) is applied to the model followed by a steady current at $-0.47 \mu\text{A}/\text{cm}^2$. Such a protocol causes the state of the model to switch from purely sub-threshold to mixed sub- and

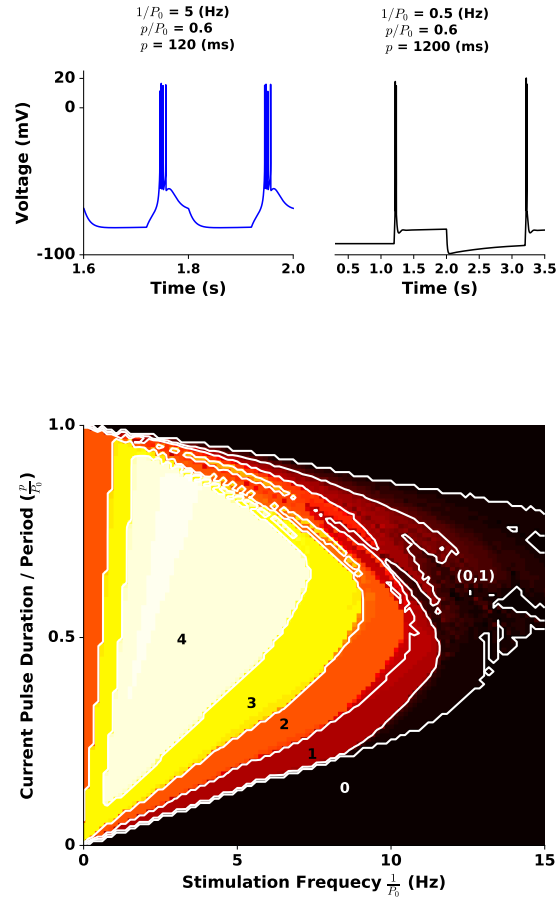


Figure 2: Responses to rhythmic hyperpolarizations. We stimulate the model given in Table 4 using a periodic pulse with frequency ($\frac{1}{P_0}$) varying from 0.1 to 15 Hz. **Upper panels** show the results of two simulations out of 100×100 . The blue curve indicates bursts of four spikes ($\frac{1}{P_0} = 5$ Hz and $\frac{p}{P_0} = 0.6$). Black curve depicts a case of two spikes bursts ($\frac{1}{P_0} = 0.5$ Hz and $\frac{p}{P_0} = 0.6$). **Bottom panel** shows the average number of spikes (sub- or supra-threshold) measured per pulse. Frequency varies in the interval $[0.1, 15]$ Hz and the ratio $\frac{p}{P_0}$ is in interval $[0, 1]$. Numbers signify the average number of spikes per pulse.

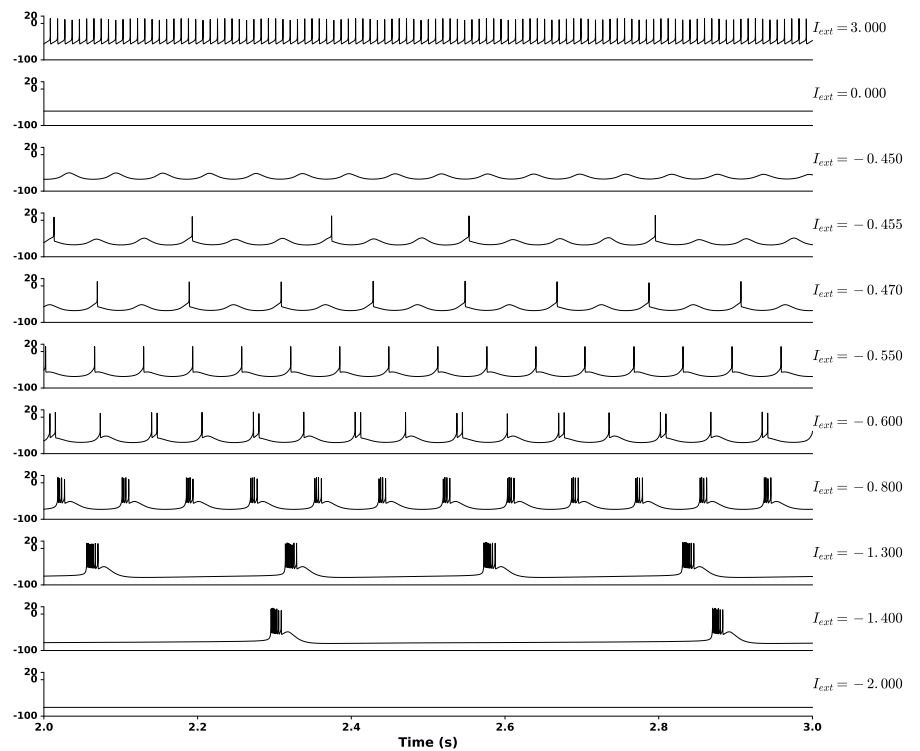


Figure 3: Dynamic behavior of neuron. Eleven different external constant currents $I_{app} = 3.0, 0.0, -0.45, -0.455, -0.47, -0.55, -0.6, -0.8, -1.3, -1.4, -2.0 \mu\text{A}/\text{cm}^2$ have been applied as inputs to the model described by equations given in Table 4. The behavior of the model spans from tonic spiking to spikes bursts, subthreshold activity and no activity at all.

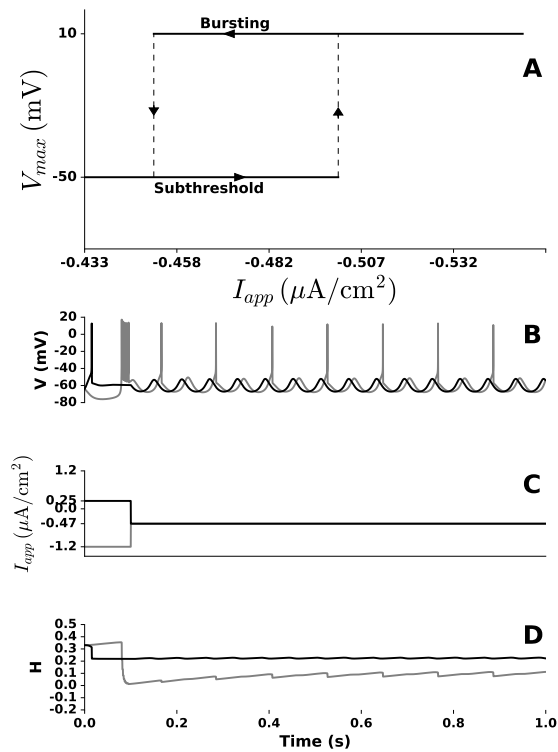


Figure 4: Hysteresis near the transition from the subthreshold to bursting oscillation. (A) Hysteresis diagram indicates a coexistence of bursting and subthreshold activity. (B) Bistability example shows how the same system can produce either subthreshold activity (black curve) or burst activity (gray curve). (C) shows the activation of H for the same simulation as in the panel above. (D) A brief current pulse at $0.25 \mu\text{A}/\text{cm}^2$ (black curve) or $-1.2 \mu\text{A}/\text{cm}^2$ (gray curve) followed by a steady current at $-0.47 \mu\text{A}/\text{cm}^2$ is used as external input to the model.

suprathreshold. These results are illustrated in Figure 4 **B**. In the same figure panels **C** and **D** depict the input to the model and the H of the Sag channel, respectively.

Another interesting behavior of the model is the development of “spiral” chaos (see Fig 6 in [4]). In this case the external input is constant and its amplitude is set to $-0.95 \mu\text{A}/\text{cm}^2$. The results for this case are shown in Figure 5, and the current model is capable of generating “spiral” chaos as in [4].

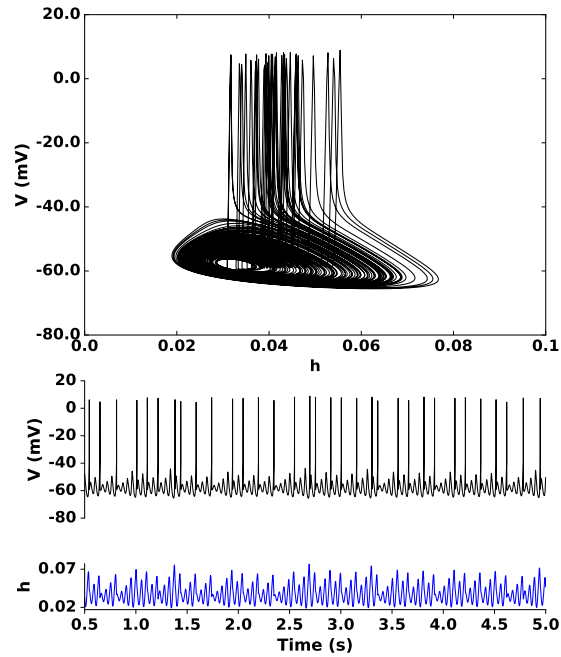


Figure 5: “Spiral Chaos”. It is generated when a constant current with amplitude $-0.95 \mu\text{A}/\text{cm}^2$ is injected to the model described in Table 4 and using the parameters from Table 5. **Top panel** shows the phase portrait of the membrane potential and the Sag current (V vs h). **Middle panel** illustrates the membrane potential (V) and, the **bottom panel** shows the h current over time.

The bursting frequency of the model can be affected by the injected external current (see Fig 7 in [4], two bursting modes). To verify that the present implementation is capable of producing similar results we captured data² values for the external current from Fig 7 of the original article (dots in Fig 7, pg. 27 in [4]) using a software called PlotDigitizer³. So for every data point (external current amplitude), we ran a simulation and the bursting frequency of the membrane potential was measured. The results are illustrated in Figure 6. The black curve shows the frequency in Hz and the blue curve shows the period in sec. Black dots indicate the frequency and open circles the corresponding period (present implementation), respectively. Cyan crosses show the original data taken from [4] and magenta pentagons the corresponding period. It is apparent that the present implementation is able to reproduce Wang’s Fig 7, despite the fact that some of the original points do not match the exactly the ones computed using the reference implementation code. Furthermore, it is worth mentioning that for properly replicate Figure 6 we had to run quite long simulations (see Table 2). If the signal is too short the results can be quite different from the ones given in [4].

Fig 2 of [4] illustrates an “intermittent” phase-locking phenomenon, generated by integrating the model described in Table 4 and using a periodic pulse with frequency

²Data are available in the accompanying github repository of the present article.

³(<http://plotdigitizer.sourceforge.net/>)

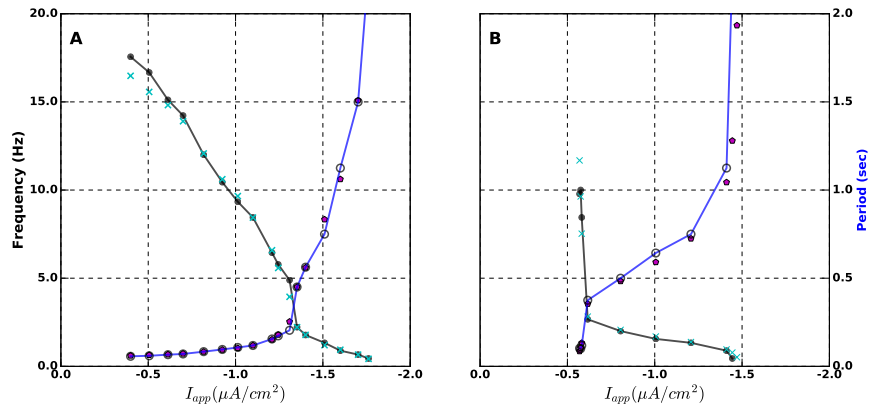


Figure 6: Frequency and period versus steady input current. This figure illustrates how an external current (ranging from 0 to $-2 \mu\text{A}/\text{cm}^2$ affects the bursts frequency (bursting mode) of the model. Black curve indicates frequency (black dots) in Hz and blue curve period (white circle discs) in sec. Cyan crosses (frequency) and magenta pentagons (period) indicate original data extracted from [4].

10 Hz and ratio $\frac{p}{P_0} = 0.8$ as external current. We applied the same protocol on the current implementation by using six different amplitude values and two different T-type calcium conductance values. $I_{app} = -1.4, -1.5, -1.6 \mu\text{A}/\text{cm}^2$ and $g_T = 0.3 \text{ mS}/\text{cm}^2$ $I_{app} = -1.2, -1.5, -1.8 \mu\text{A}/\text{cm}^2$ and $g_T = 0.25 \text{ mS}/\text{cm}^2$. After counting sub- and supra-threshold spikes, we computed the symbolic patterns for every simulation. Figure 7 shows 2 seconds of membrane potential for every simulation along with symbolic patterns of 0 (dark circles) and 1 (green line segments). Results given in Figure 7 are similar to the ones of Fig 2A and Fig 2B.

Conclusion

A conductance-based model for relay thalamocortical neurons proposed by [4] was implemented in Python. The present model was tested thoroughly by using several examples from the original article. In general, the original model is easily implemented since all the equations and most of the parameters (except the initial time step of the integration method) are given. However, in some experimental protocols important information is missing (e.g. Wang’s Fig 1 in [4], where our results do not match exactly the original ones), leading to a less faithful reproduction of those results. Furthermore, to the best of our knowledge, no any other implementation of [4] is available the thus we cannot compare the current implementation to any other.

References

- [1] Uri M Ascher and Linda R Petzold. *Computer methods for ordinary differential equations and differential-algebraic equations*. Vol. 61. Siam, 1998.
- [2] DA McCormick and HR Feuser. “Functional implications of burst firing and single spike activity in lateral geniculate relay neurons”. In: *Neuroscience* 39.1 (1990), pp. 103–113.
- [3] Eilen Nordlie, Marc-Oliver Gewaltig, and Hans Ekkehard Plesser. “Towards reproducible descriptions of neuronal network models”. In: *PLoS Comput Biol* 5.8 (2009), e1000456.
- [4] X-J Wang. “Multiple dynamical modes of thalamic relay neurons: rhythmic bursting and intermittent phase-locking”. In: *Neuroscience* 59.1 (1994), pp. 21–31.

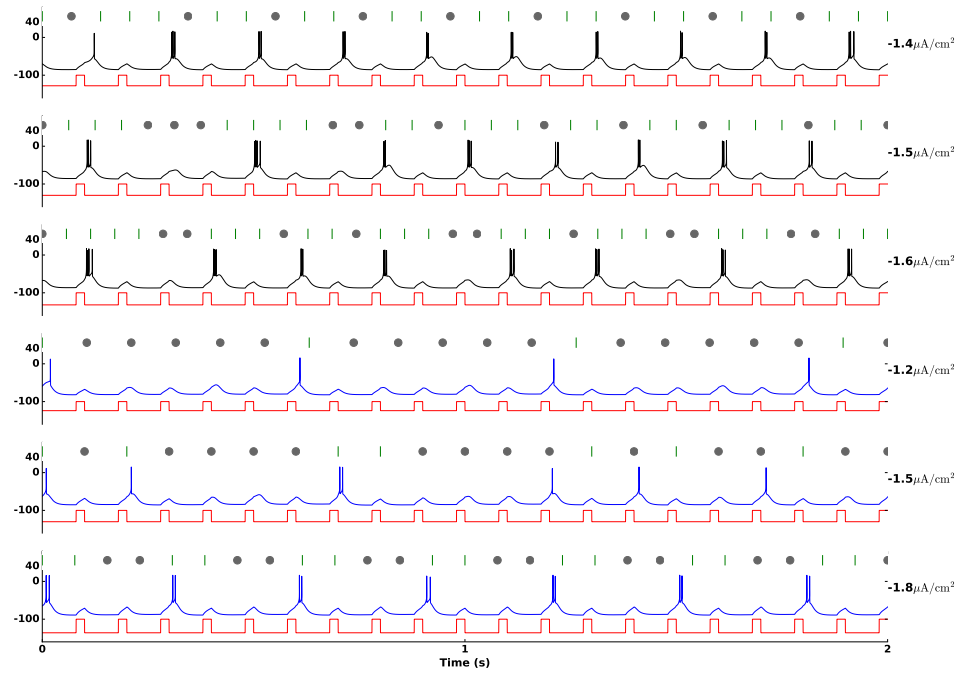


Figure 7: Symbolic patterns. Six different simulations are illustrated here ($I_{app} = -1.4, -1.5 - 1.6 \mu\text{A}/\text{cm}^2$ with $g_T = 0.3 \text{ mS}/\text{cm}^2$) and ($I_{app} = -1.2, -1.5, -1.8 \mu\text{A}/\text{cm}^2$ with $g_T = 0.25 \text{ mS}/\text{cm}^2$). Symbolic patterns are illustrated above membrane potential traces as green line segments – suprathreshold spikes and dark circles – subthreshold spikes. Red curve indicates the input periodic pulses.